Zigzag Ribbons

DOI: 10.1002/anie.201403302

Synthesis of Nitrogen-Doped ZigZag-Edge Peripheries: Dibenzo-9*a*-azaphenalene as Repeating Unit**

Reinhard Berger, Angelos Giannakopoulos, Prince Ravat, Manfred Wagner, David Beljonne, Xinliang Feng,* and Klaus Müllen**

Abstract: *A bottom-up approach toward stable and monodisperse segments of graphenes with a nitrogen-doped zigzag edge is introduced. Exemplified by the so far unprecedented dibenzo-9a-azaphenalene (DBAPhen) as the core unit, a versatile synthetic concept is introduced that leads to nitrogen-doped zigzag nanographenes and graphene nanoribbons.*

Phenalene (**1**) is the prototype of a non-Kekulé polycyclic aromatic hydrocarbon (PAH).[1] It can occur as a neutral, delocalized radical with 13 π electrons as well as an anionic (14 π e^-) or a cationic (12 π e^-) aromatic compound.[2] Being the smallest D_{3h}-symmetric PAH after benzene, it is a structural motif for graphene that has entirely zigzag-edge peripheries. Repetition of this motif can lead to nanographenes or graphene nanoribbons (GNRs) that have entirely zigzag edges.[3] In contrast to the fully benzenoid nanographenes or GNRs,[4] segments of graphene with zigzag peripheries have unpaired electrons primarily located on the edges.[5] These zigzag graphenes are candidates for spintronics.[6] However, they are kinetically unstable in terms of oxidation or dimerization,[1b,7] and the synthesis of larger monodisperse, open-shell zigzag-graphene segments remains a challenging task, the so-called "synthetic organic spin chemistry".[8]

Here, we introduce the synthesis of 9*a*-azaphenalenes **5** and **6** (Figure 1) with dibenzo-elongated zigzag edges and propose a procedure for the solution-based bottom-up approach towards doped zigzag GNRs. This is exemplified on the next higher homologue **7**, an aza derivative of dibenzoheptazethrene synthesized by Clar et al.[9] In contrast to previously studied azaphenalenes, such as 9*b*-azaphenalene (cyclazine) (**2**)[10] and 1-azaphenalene (**3**),[11] the introduction of nitrogen into the zigzag edge results in a neutral diradical **4a**. This can, in principle, be stabilized in a zwitterionic valence bond structure of an azomethine ylide (AMY) type **4b.**[12] The high chemical reactivity of the nitrogen "doping" at the 9*a*-position is demonstrated by the dimerization and the [2+3] cycloaddition reaction of the in situ created *t*Bu-DBAPhen **5**. Single-crystal analysis revealed the selective addition of dimethyl acetylenedicarboxylate (DMAD) to the AMY side of **5**. A bulky aryl group was introduced in **6** to cause steric shielding of the highly reactive periphery in **5** and so inhibit self-dimerization and increase the kinetic stability.

The synthesis of **5** and **6** was accomplished by treatment of the corresponding precursor derivatives **11** and **12** with base. These precursors can all be derived from **8** (Scheme 1). The synthesis of the precursor comprises the following steps: First, Suzuki coupling was performed between 2,6-dibromo-4-(*tert*-butyl)aniline (**8**) and 1-hydroxy-3*H*-2,1-benzoxaborole (**9**) to afford **10** or **13**, and a repeated Suzuki coupling of **13** and l,5-dibora-2,6-dioxa-*sym*-hydrindacene-l,5-diol (**14**)[13] led to **15**. Second, a HCl-induced microwave-assisted, cyclization of **10** and **15** afforded precursors **11** and **16**, while further Grignard addition and hydride abstraction from **11** provided **12** with a phenyl-terminated edge.

[*] R. Berger, P. Ravat, Dr. M. Wagner, Prof. Dr. X. Feng, Prof. Dr. K. Müllen
Max-Planck-Institut für Polymerforschung
Ackermannweg 10, 55128 Mainz (Germany)
E-mail: feng@mpip-mainz.mpg.de
muellen@mpip-mainz.mpg.de
A. Giannakopoulos, Dr. D. Beljonne
Chimie des Matériaux Nouveaux &
Centre d'Innovation et de Recherche en Matériaux Polymères
Université de Mons- UMONS/Materia Nova
Place du Parc 20, 7000 Mons (Belgium)
E-mail: david.beljonne@umons.ac.be

[**] We acknowledge support by the EC Graphene Flagship (contract no. CNECT-ICT-604391) and ERC Nanograph. We thank Dr. Schollmeyer (University of Mainz) for X-ray crystal-structure analysis. R.B. thanks the Fond der Chemischen Industrie for a Chemiefonds fellowship. A.G. acknowledges funding from the 7th Marie Curie ITN GENIUS program and the OPTI2MAT Excellence Program of Région Wallonne and FNRS/FRFC. D.B. is a research director of the Fonds National de la Recherche Scientifique-FNRS.

Supporting information for this article is available on the WWW under http://dx.doi.org/10.1002/anie.201403302.

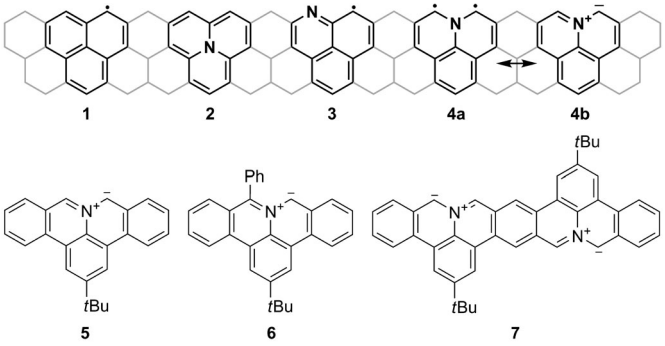

Figure 1. Phenalene **1** and aza derivatives **2**–**4**; dibenzoazaphenalenes **5** and **6** and their repeated structural motif in dimer **7**.

Although the cyclization of **10** was conducted in the presence of oxygen under harsh conditions (HCl, 130 °C, 6 bar), no decomposition by oxidation or polymerization was observed, and **11** was obtained in 99 % yield by precipitation. The selective α-addition of phenylmagnesium bromide to **11**

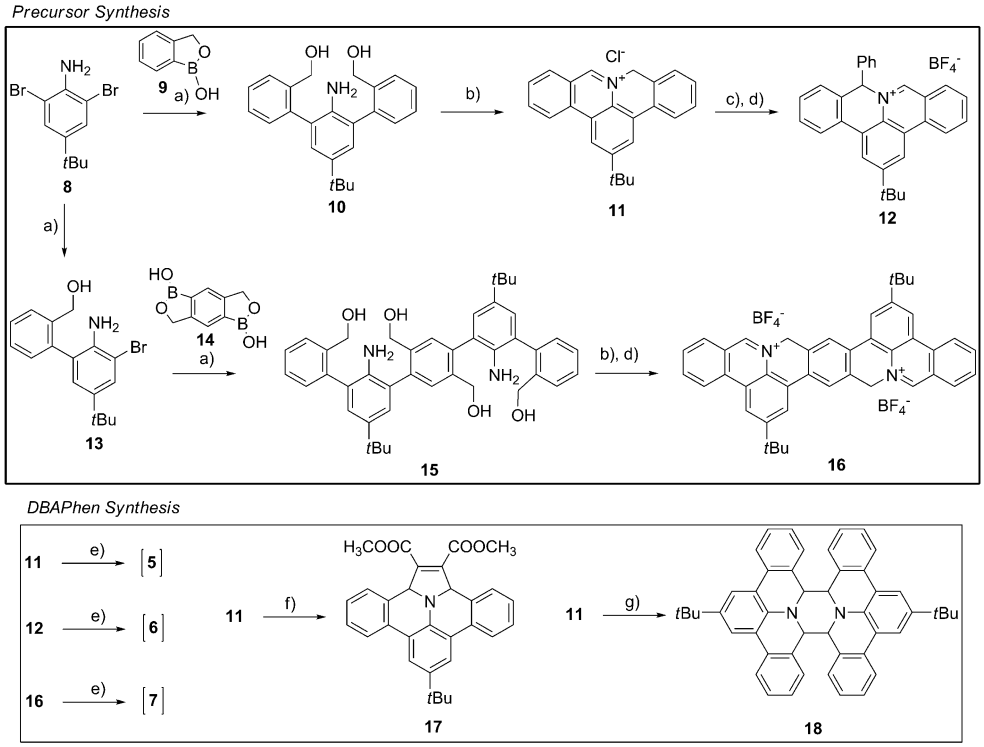

Scheme 1. Synthesis of precursors **11**, **12**, and **16**, and in situ generation of DBAPhens **5**–**7**. Trapping of **5** by either a [3+2] cycloaddition reaction in the presence of dimethoxyacetylene dicarboxylate (DMAD) to **17**, or by dimerization to **18**. a) $[Pd(PPh_3)_4]$, K_2CO_3 (2 M), toluene, ethanol; b) HCl in dioxane (4 M), microwave, O_2, 99%; c) PhMgBr, THF, 0°C; d) trityl BF_4, toluene, acetonitrile, 90°C; e) TEA; f) DMAD, TEA, CH_2Cl_2, 25°C, 53%; g) DMSO, NBu_3, 190°C, 51%.

and hydride abstraction by trityl tetrafluoroborate at 90°C resulted in the kinetically controlled Hofmann product **12** with the phenyl substituent on the saturated α-carbon atom (see Figure S2 in the Supporting Information). The stable, charged precursors **11**, **12**, and **16** are readily soluble in polar organic solvents and thus can be purified by repeated precipitation in *n*-hexane. Finally, deprotonation of precursors **11, 12**, and **16** by using anhydrous triethylamine (TEA) generated solutions of **5**–**7** under inert conditions.

As **5**–**7** could not be isolated, due to their high reactivity, a solution of **5** was prepared and trapped with DMAD to afford the [3+2] cycloaddition product **17**. Interestingly, in the absence of the trapping reagent DMAD, work-up of the resulting mixture gave the dimerized compound **18** in 3% yield. Such a dimerization reaction actually has also been observed for other AMYs.[14] Preheating solutions of precursor **11** at 190°C prior to the addition of the high-boiling base tributylamine led to **18** in 51% yield. All intermediates and precursor compounds were analyzed by ^1H and ^{13}C NMR spectroscopy as well as HRESI mass spectroscopy. The ^1H NMR spectra of in situ prepared solutions of **6** showed complete conversion of the precursor **12**, as evident, for example, by the disappearance of the characteristic iminium proton at $\delta = 10.3$ ppm. A resolved spectrum could not be obtained even if the sample was prepared and measured at −60°C. Nevertheless, the observed signals in the ^1H NMR spectrum strongly suggests the zwitterionic structure of **6** (see Figure S6 in the Supporting Information). The majority of AMYs cannot be characterized by ^1H NMR spectroscopy because of their high reactivity, and only a few isolable AMYs have been reported in the literature.[15] X-ray analysis of single crystals of the cycloadduct **17** grown by slow evaporation of solutions in dichloromethane (Figure 2) clearly reveals selective addition to the 1,3-positions of the AMY site. The structure of the dimer **18** was also confirmed by NMR spectroscopy and HR-ESI MS.

The UV/Vis absorption spectra of **5**–**7** were recorded in situ under inert conditions (Figure 2c). The generation of **5** and **6** results in broad absorptions at $\lambda = 580$ nm (536 nm) arising, which demonstrate extended conjugation compared to their precursors **11** and **12**, which have maxima at $\lambda = 366$ nm

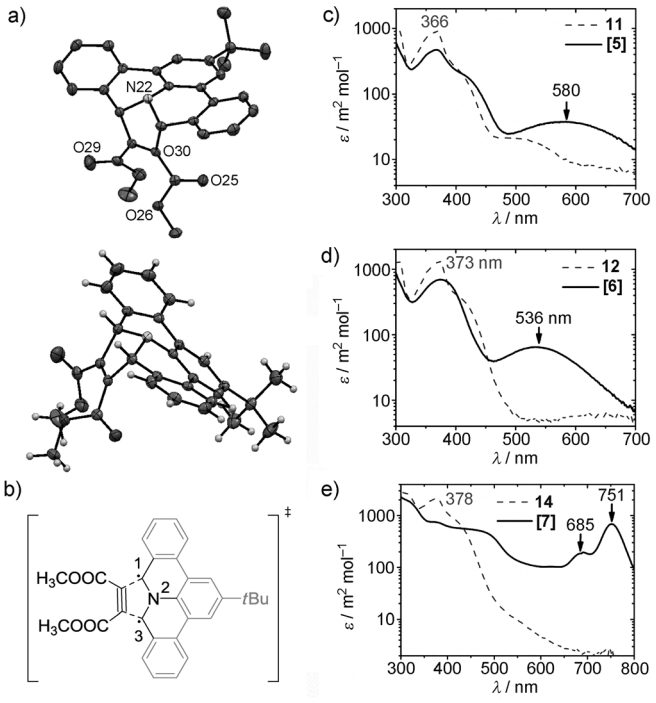

Figure 2. a) Crystal structure of cycloaddition product **17** showing selective 1,3-addition to the nitrogen side; b) proposed transient state of [2+3] cycloaddition reaction between DBAPhen **5** and DMAD; c)–e) UV/Vis absorption of precursors (dashed lines) **11**, **12**, and **16**, as well as in situ generated solutions of DBAPhens **5**, **6**, and **7** in CH_2Cl_2 immediately after addition of base.

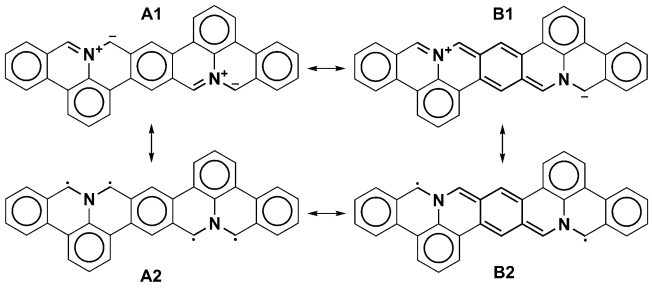

Scheme 2. Quinoid resonance stabilization between two adjacent repeating units represented in **B1** and **B2** compared to **A1** and **A2**, which possess a higher number of Clar sextets. In contrast to the closed-shell structure of **A1**, **B2** is a diradical, which indicates a stabilized open-shell state.

(378 nm). In contrast to the absorption band of **5**, that of **6** is narrower and hypsochromically shifted, which supports a localization of the negative charge on the phenyl-substituted carbon atom. The formation of **18** by dimerization of **5** results in an absorption shoulder at $\lambda = 420$ nm. A similar observation is not found for the phenyl derivative **6**. In the case of dimer **7**, an absorption maximum at $\lambda = 751$ nm is observed (for comparison: λ(heptacene) = 728 nm).[15] This large bathochromic shift of the absorption of **7** compared to those of **5** and **6** stems not only from the extended conjugation in the two mesomeric structures **A1** and **A2** (Scheme 2), but also by an additional quinoid resonance stabilization of the two nitrogen centers in **B1** and **B2**.

We have used density functional theory (DFT) with the hybrid functional HSEH1PBE and the 6-31G(d) basis set to investigate the evolution of the geometric and electronic structures upon oligomerization of monomer (**5**) to tetramer (**ttm**) in the singlet (triplet) state (Figure 3a). The lowest singlet electronic excited states and the linear optical absorption spectra of the oligomers were also computed at the TD-DFT and AM1/CIS levels. An HSEH1PBE ESP charge analysis yields large positive charges of about 0.35 |e| on the nitrogen atoms and negative charges of about −0.23 |e| on the neighboring CH units (see Figure S8 in the Supporting Information), which is consistent with a sizeable ionic contribution in the ground state. In addition, the nitrogen–carbon bond lengths of about 1.36 Å indicate a close to double-bond character, in line with the zwitterionic **A1** form in Scheme 2. The equilibrium geometry suggests a predominant Clar formula with aromatic sextets delocalized in a zigzag orientation with respect to the longitudinal axis of the molecules, as exemplified for **tm** in Figure 3b. This is borne out by the bonding-antibonding pattern in the HOMO (Figure 3c, left). Notice in particular the clear aromatic character of the benzene rings connecting the nitrogen-doped units and the presence of localized contributions to the HOMO wave functions on the carbon sites adjacent to the nitrogen atoms. There is a one-to-one correspondence between the electronic density in the HOMO and the radical form **A2** (Scheme 2). Likewise, the excess spin density in the triplet state shows dominant contributions from the carbon atoms bonded to the nitrogen atoms at the ribbon edges, as shown for **tm** (Figure 3d).

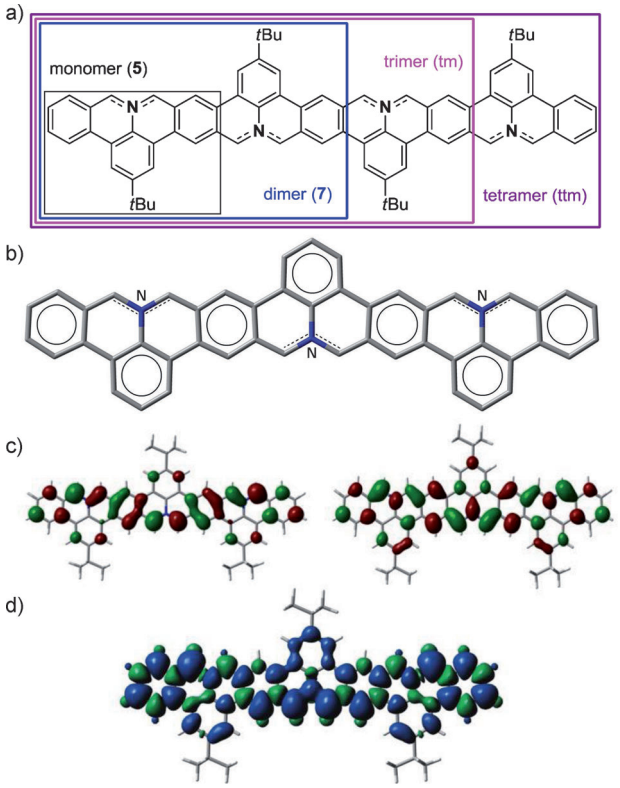

Figure 3. a) Chemical structures of the trimer (**tm**) and tetramer (**ttm**). b) Equilibrium geometry of **tm**. N–C bond lengths (dahed lines, $d_{C\text{-}N} = 1.36$ Å) indicate a close to double-bond character in line with the **A1** form (Scheme 2). c) Molecular orbitals of **tm**. Left: HOMO; right: LUMO. d) Spin density plot of the triplet state of **tm**.

Altogether, we can conclude that the ground-state structure of the representative oligomers **7** to **ttm** can be accounted for by the superimposition of the ionic and radical aromatic Clar formulas **A1** and **A2** (Scheme 2). Note also that: 1) the shape of the LUMO orbital of **ttm** (Figure 3c, right), with a quinoidic pattern on the connecting benzene rings, is more consistent with Clar's formulas **B1** and **B2**; and that 2) the ground state of all the representative molecules investigated is singlet, although the singlet–triplet energy spacing reduces from about 1 eV in the monomer **5** to about 0.2 eV in the tetramer (**ttm**). This is in agreement with the EPR spectroscopic analysis of **6** at a concentration of 10^{-4} mol L^{-1} not showing any signal.

The UV/Vis spectra of **5**, **7**, and **tm** have been computed at the TD-DFT and AM1/CIS levels (see Figures S19–S21 in the Supporting Information). For the monomer **5**, both methods indicate two main absorption bands in the low-energy spectral domain, with the lowest electronic transition carrying much smaller oscillator strength. On the basis of their relative intensity and energetic position, we assign these two bands to the features measured at $\lambda \approx 380$ and 540 nm (Figure 2c). As the molecular backbone gets longer (in **tm**), the lowest optical transition acquires a dominant HOMO–LUMO character, which translates into a large bathochromic and hyperchromic shift (see Figure S21 in the Supporting Information). Both theoretical methods predict a large reduction in the optical

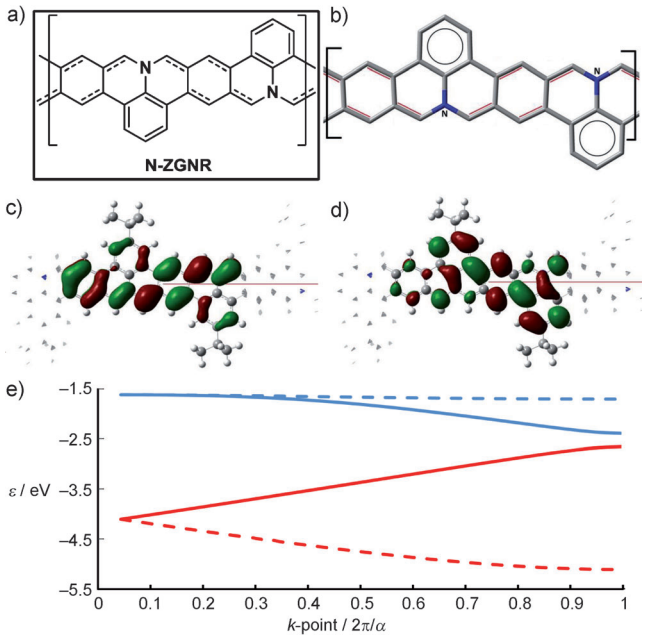

Figure 4. a) Chemical structure and b) equilibrium geometry of infinite ribbon **N-ZGNR**. The bond lengths (red lines, $d = 1.37$ Å) are in line with the quinoid structures **B1** and **B2** (Scheme 2). c,d) Molecular orbitals of **N-ZGNR** at the end of the valence and conduction band ($k = 2\pi/\alpha$). Left: HOCO; right: LUCO. e) Band structure of **N-ZGNR**. Frontier bands are shown: HOCO-1 (dotted red), HOCO (red), LUCO (blue), and LUCO + 1 (dotted blue).

gap as the ribbons get longer, in line with the experimental results.

Based on these findings, it is useful to extrapolate the data obtained for the oligomers **7-ttm** to the corresponding infinite ribbon **N-ZGNR** (Figure 4a). A linear fit to the HOMO–LUMO gap as a function of inverse length yields a bandgap of about 0.23 eV. This is in good agreement with spin-polarized DFT calculations on the electronic band structure, which provide a bandgap of about 0.26 eV (Figure 4e). The frontier HOCO (highest occupied crystalline orbital) and LUCO (lowest unoccupied crystalline orbital) show a large dispersion, at odds with the typical flat bands associated with edge states in zigzag ribbons. The comparison with pristine **ZGNR** is shown in the Supporting Information (see Figures S15–S18).

In summary, a bottom-up approach towards nitrogen-doped zigzag GNRs was introduced based on the synthesis of the unprecedented DBAPhen **5**. The key step is the deprotonation of a stable, soluble precursor **10**, which allows formation of the sensitive zigzag edge in **5** under mild and inert conditions. The possibility of lateral extension towards nitrogen-doped zigzag GNRs was demonstrated by the synthesis of its dimer **7**. The repetition of the structural motif leads to a strong bathochromic and hyperchromic shift. DFT calculations predict the evolution of the geometric and electronic properties upon oligomerization into an infinite nitrogen-doped zigzag ribbon **N-ZGNR**. Extension towards precursor polymers through the same synthetic procedure is straightforward, and further stabilization of the nitrogen-doped zigzag periphery is currently being pursued to obtain stable nitrogen-doped zigzag GNRs by a solution approach. Importantly, the high chemical reactivity of the 9*a*-azaphenalene results in it having the potential to be a powerful building block for the synthesis of larger nitrogen-containing polycyclic aromatic hydrocarbons.

Received: March 13, 2014
Published online: August 11, 2014

Keywords: azomethine ylides · graphene nanoribbons · organic radicals · phenalenes · polycyclic aromatic hydrocarbons

[1] a) W. Klyne, R. Robinson, *J. Chem. Soc.* **1938**, 1991–1994; b) F. Gerson, *Helv. Chim. Acta* **1966**, *49*, 1463–1467; c) P. B. Sogo, M. Nakazaki, M. Calvin, *J. Chem. Phys.* **1957**, *26*, 1343–1345; d) D. H. Reid, *Tetrahedron* **1958**, *3*, 339–352.

[2] a) G. D. O'Connor, T. P. Troy, D. A. Roberts, N. Chalyavi, B. Fückel, M. J. Crossley, K. Nauta, J. F. Stanton, T. W. Schmidt, *J. Am. Chem. Soc.* **2011**, *133*, 14554–14557; b) M. K. Cyrański, R. W. A. Havenith, M. A. Dobrowolski, B. R. Gray, T. M. Krygowski, P. W. Fowler, L. W. Jenneskens, *Chem. Eur. J.* **2007**, *13*, 2201–2207.

[3] a) Y. Li, K.-W. Huang, Z. Sun, R. D. Webster, Z. Zeng, W. Zeng, C. Chi, K. Furukawa, J. Wu, *Chem. Sci.* **2014**, *5*, 1908–1914; b) Y. Li, W.-K. Heng, B. S. Lee, N. Aratani, J. L. Zafra, N. Bao, R. Lee, Y. M. Sung, Z. Sun, K.-W. Huang, R. D. Webster, J. T. López Navarrete, D. Kim, A. Osuka, J. Casado, J. Ding, J. Wu, *J. Am. Chem. Soc.* **2012**, *134*, 14913–14922.

[4] a) S. Xiao, S. J. Kang, Y. Wu, S. Ahn, J. B. Kim, Y.-L. Loo, T. Siegrist, M. L. Steigerwald, H. Li, C. Nuckolls, *Chem. Sci.* **2013**, *4*, 2018–2023; b) A. Narita, X. Feng, Y. Hernandez, S. A. Jensen, M. Bonn, H. Yang, I. A. Verzhbitskiy, C. Casiraghi, M. R. Hansen, A. H. R. Koch, G. Fytas, O. Ivasenko, B. Li, K. S. Mali, T. Balandina, S. Mahesh, S. De Feyter, K. Müllen, *Nat. Chem.* **2014**, *6*, 126–132; c) C.-A. Palma, K. Diller, R. Berger, A. Welle, J. Björk, J. L. Cabellos, D. J. Mowbray, A. C. Papageorgiou, N. P. Ivleva, S. Matich, E. Margapoti, R. Niessner, B. Menges, J. Reichert, X. Feng, H. J. Räder, F. Klappenberger, A. Rubio, K. Müllen, J. V. Barth, *J. Am. Chem. Soc.* **2014**, *136*, 4651–4658; d) F. Schlütter, T. Nishiuchi, V. Enkelmann, K. Müllen, *Angew. Chem. Int. Ed.* **2014**, *53*, 1538–1542; *Angew. Chem.* **2014**, *126*, 1564–1568; e) X. Yang, X. Dou, A. Rouhanipour, L. Zhi, H. J. Räder, K. Müllen, *J. Am. Chem. Soc.* **2008**, *130*, 4216–4217; f) M. G. Schwab, A. Narita, Y. Hernandez, T. Balandina, K. S. Mali, S. De Feyter, X. Feng, K. Müllen, *J. Am. Chem. Soc.* **2012**, *134*, 18169–18172; g) L. Dössel, L. Gherghel, X. Feng, K. Müllen, *Angew. Chem. Int. Ed.* **2011**, *50*, 2540–2543; *Angew. Chem.* **2011**, *123*, 2588–2591; h) L. Chen, Y. Hernandez, X. Feng, K. Müllen, *Angew. Chem. Int. Ed.* **2012**, *51*, 7640–7654; *Angew. Chem.* **2012**, *124*, 7758–7773.

[5] a) L. Talirz, H. Söde, J. Cai, P. Ruffieux, S. Blankenburg, R. Jafaar, R. Berger, X. Feng, K. Müllen, D. Passerone, R. Fasel, C. A. Pignedoli, *J. Am. Chem. Soc.* **2013**, *135*, 2060–2063; b) A. Konishi, Y. Hirao, K. Matsumoto, H. Kurata, R. Kishi, Y. Shigeta, M. Nakano, K. Tokunaga, K. Kamada, T. Kubo, *J. Am. Chem. Soc.* **2013**, *135*, 1430–1437; c) A. Konishi, Y. Hirao, M. Nakano, A. Shimizu, E. Botek, B. Champagne, D. Shiomi, K. Sato, T. Takui, K. Matsumoto, H. Kurata, T. Kubo, *J. Am. Chem. Soc.* **2010**, *132*, 11021–11023; d) S. Banerjee, D. Bhattacharyya, *Comput. Mater. Sci.* **2008**, *44*, 41–45; e) K. Nakada, M. Fujita, G. Dresselhaus, M. S. Dresselhaus, *Phys. Rev. B* **1996**, *54*, 17954–17961.

[6] a) J. Ferrer, V. M. Garcia-Suarez, *J. Mater. Chem.* **2009**, *19*, 1696–1717; b) J. Ferrer, V. M. Garcia-Suarez, *J. Mater. Chem.*

2009, *19*, 1670 – 1671; c) R. C. Haddon, *Nature* **1975**, *256*, 394 – 396.
[7] P. A. Koutentis, Y. Chen, Y. Cao, T. P. Best, M. E. Itkis, L. Beer, R. T. Oakley, A. W. Cordes, C. P. Brock, R. C. Haddon, *J. Am. Chem. Soc.* **2001**, *123*, 3864 – 3871.
[8] a) Y. Morita, S. Suzuki, K. Sato, T. Takui, *Nat. Chem.* **2011**, *3*, 197 – 204; b) Z. Sun, Q. Ye, C. Chi, J. Wu, *Chem. Soc. Rev.* **2012**, *41*, 7857 – 7889.
[9] E. Clar, G. S. Fell, M. H. Richmond, *Tetrahedron* **1960**, *9*, 96 – 105.
[10] a) D. Farquhar, D. Leaver, *J. Chem. Soc. D* **1969**, 24 – 25; b) M. J. S. Dewar, N. Trinajstic, *J. Chem. Soc. A* **1969**, 1754 – 1755.
[11] S. O'Brien, D. C. C. Smith, *J. Chem. Soc.* **1963**, 2907 – 2917.
[12] B. Braida, C. Walter, B. Engels, P. C. Hiberty, *J. Am. Chem. Soc.* **2010**, *132*, 7631 – 7637.
[13] J. F. Cairns, H. R. Snyder, *J. Org. Chem.* **1964**, *29*, 2810 – 2812.
[14] a) P. V. Guerra, V. A. Yaylayan, *J. Agric. Food Chem.* **2010**, *58*, 12523 – 12529; b) F. Freeman, G. Govindarajoo, *Rev. Heteroat. Chem.* **1995**, *13*, 123 – 147.
[15] a) E. Lopez-Calle, M. Keller, W. Eberbach, *Eur. J. Org. Chem.* **2003**, 1438 – 1453; b) Y. Kobayashi, I. Kumadaki, T. Yoshida, *Heterocycles* **1977**, *8*, 387 – 390; c) J. P. Freeman, *Chem. Rev.* **1983**, *83*, 241 – 261; d) H. Seidl, R. Huisgen, R. Knorr, *Chem. Ber.* **1969**, *102*, 904 – 914.

